ELSEVIER

Cell Calcium 43 (2008) 107–121

cell calcium

www.elsevier.com/locate/ceca

Mechanism of acetylcholine-induced calcium signaling during neuronal differentiation of P19 embryonal carcinoma cells *in vitro*

Rodrigo R. Resende [a], Katia N. Gomes [a], Avishek Adhikari [a,1], Luiz R.G. Britto [b], Henning Ulrich [a,*]

[a] *Departamento de Bioquímica, Instituto de Química, Universidade de São Paulo, Av. Prof. Lineu Prestes 748, 05508-900 São Paulo, SP, Brazil*
[b] *Departamento de Fisiologia e Biofísica, Instituto de Ciências Biomédicas, Universidade de São Paulo, Paulo, 05508-900 São Paulo, SP, Brazil*

Received 26 September 2006; received in revised form 12 April 2007; accepted 13 April 2007
Available online 26 July 2007

Abstract

Muscarinic (mAChRs) and nicotinic acetylcholine receptors (nAChRs) are involved in various physiological processes, including neuronal development. We provide evidence for expression of functional nicotinic and muscarinic receptors during differentiation of P19 carcinoma embryonic cells, as an *in vitro* model of early neurogenesis. We have detected expression and activity of α_2–α_7, β_2, β_4 nAChR and M1–M5 mAChR subtypes during neuronal differentiation. Nicotinic α_3 and β_2 mRNA transcription was induced by addition of retinoic acid to P19 cells. Gene expression of α_2, α_4–α_7, β_4 nAChR subunits decreased during initial differentiation and increased again when P19 cells underwent final maturation. Receptor response in terms of nicotinic agonist-evoked Ca^{2+} flux was observed in embryonic and neuronal-differentiated cells. Muscarinic receptor response, merely present in undifferentiated P19 cells, increased during neuronal differentiation. The nAChR-induced elevation of intracellular calcium ($[Ca^{2+}]_i$) response in undifferentiated cells was due to Ca^{2+} influx. In differentiated P19 neurons the nAChR-induced $[Ca^{2+}]_i$ response was reduced following pretreatment with ryanodine, while the mAChR-induced response was unaffected indicating the contribution of Ca^{2+} release from ryanodine-sensitive stores to nAChR- but not mAChR-mediated Ca^{2+} responses. The presence of functional nAChRs in embryonic cells suggests that these receptors are involved in triggering Ca^{2+} waves during initial neuronal differentiation.

Keywords: Neuronal differentiation; P19 embryonal carcinoma cells; Acetylcholine receptors; Ryanodine receptors; IP_3 receptors; Ca^{2+} signaling

1. Introduction

The development of the nervous system is one of the most important morphogenetic events occurring in the embryo. This process is accompanied by cell proliferation and differentiation as well as by tissue organization into a specific architecture. Although the specific molecular pathways that drive these events remain unresolved, it is widely believed that proliferation and differentiation programs of the neural progenitors require the interaction of extrinsic and intrinsic signals. While the function of growth factors in controlling neuronal differentiation is well documented, there also is increasing persuasive evidence for a role of neurotransmitters and their respective receptors in this process [1,2]. Many neurotransmitters are already present in the brain prior to axonogenesis and synaptogenesis, raising the possibility that they may mediate non-classical signaling. One such neurotransmitter is acetylcholine (ACh), whose biological actions are mediated by both nicotinic (nAChRs) and muscarinic receptors (mAChRs). Neuronal nAChRs are heterogeneous, with at least six α (α_2–α_7) and three β (β_2–β_4) subunits (reviewed in [3]). Nicotinic receptor subunits are among the first membrane proteins to appear during central nervous system (CNS) development, and their initial expression does not

* Corresponding author. Tel.: +55 11 3091 3810x223; fax: +55 11 3815 5579.
E-mail address: henning@iq.usp.br (H. Ulrich).
[1] Present address: Department of Biological Sciences, Columbia University, Amsterdam Av. 1212, New York, NY 10027, USA.

0143-4160/$ – see front matter © 2007 Elsevier Ltd. All rights reserved.
doi:10.1016/j.ceca.2007.04.007

depend on nerve contact [4]. Prior to innervation, nAChRs are diffusely distributed throughout the nerve fibre surface, while after innervation, nAChRs cluster at high concentrations at neuronal junctions [5–8]. Gene expression patterns and several functional properties of nAChRs change during differentiation and maturation of neurons [9,4,10,11]. Transcription of mRNAs coding for nAChR subunits and expression of α_3, α_4, α_7, β_2, and β_4 nicotinic receptor subunits in the developing rat from early embryonic through postnatal developmental stages [4] and during *in vitro* differentiation of a P19 mouse embryonic carcinoma (EC) cell line as a model for early development [12] point at a pivotal role during the onset of neurogenesis.

In contrast to nAChRs which directly participate in neurotransmission in mature neurons, muscarinic receptor function is predominately linked to modulation of synaptic activity. Five mAChR subtypes are present in the CNS, with the M5 subtype being exclusively expressed in the brain. These receptors activate multiple signaling pathways that are important for modulating neuronal excitability, synaptic plasticity and feedback regulation of ACh release [13]. Muscarinic receptor participation in neurogenesis has been suggested based on experimental evidence. For instance, treatment of neural stem and progenitor cells with ACh or its stable analogue carbamoylcholine led to increases in DNA synthesis and accelerated neurogenesis [14]. In another study a neuroblastoma cell line, which by itself does not synthesize ACh, was transfected with a construct coding for expression of choline acetyltransferase. The activation of ACh synthesis resulted in a higher expression of neuronal specific traits compared to untransfected control cells. The presence of mAChRs in these transfected cells indicates the presence of an autocrine loop that may be responsible for the advanced differentiation state ([15], reviewed in [16]).

In the present work, we provide evidence for the presence of functional nicotinic and muscarinic receptors during *in vitro* differentiation of P19 EC cells as a model of early embryogenesis. Neuronal differentiation of this cell line is believed to closely resemble the developmental stage of the embryonic ectoderm. The observation that in addition to differential cholinergic receptor expression, the expression of choline acetyltransferase and acetylcholine esterase with its splice variants is regulated throughout the course of differentiation [17,12,18,19], makes the P19 cell line a reliable model to study cholinergic receptor function during early neuronal development.

2. Materials and methods

2.1. Abbreviations used

4-DAMP, 4-diphenylacetoxy-*N*-methylpiperidine methiodide; ACh, acetylcholine; CICR, Ca^{2+}-induced Ca^{2+} release; CPA, cyclopiazonic acid; DMEM, Dulbecco's modified Eagle's medium; EB, embryonic bodies; EM, extracellular medium; FBS, fetal bovine serum; F_{max}, maximal fluorescence; F_{min}, minimal fluorescence; IP_3, inositol-3-phosphate; mAChR, muscarinic acetylcholine receptors; MT3, green mamba *Dendroaspis angusticeps* toxin; nAChR, nicotinic acetylcholine receptors; NF, neurofilament; PBS, phosphate-buffered saline; PLC, phospholipase C; RA, "*all-trans*" retinoic acid; RT, reverse transcription; SERCA, sarcoplasmatic/endoplasmatic reticulum Ca^{2+}-ATPase; VOOC, voltage-operated Ca^{2+} channels.

2.2. Reagents

Unless otherwise indicated, all reagents were purchased from Sigma (St. Louis, MO). Primary monoclonal antibodies are from Covance (Covance Research Products, Denver, PA), rat anti-α_3 nAChR (MRT-611R), rat anti-α_4 nAChR (MRT-613R), rat anti-α_5 nAChR (MRT-623R), mouse anti-α_7 nAChR (MMS-627R) and rat anti-β_2 nAChR (MRT-639R) and appropriate secondary biotin conjugate antibodies were used at 1/200 dilutions (Santa Cruz Biotechnology, Heidelberg, Germany). The anti-α_2, -α_6 and -β_4 antibodies were a gift from Dr. Jon Lindstrom (Department of Neuroscience, University of Pennsylvania and Philadelphia, PA). Primers for RT-PCR reactions were synthesized by Integrated DNA Technologies, Coralville, IA.

2.3. Culture and neuronal differentiation of P19 cells

P19 murine embryonal carcinoma cells were grown in DMEM (Invitrogen, Carlsbad, CA) supplemented with 10% of final volume with fetal bovine serum (FBS) (Cultilab, Campinas, Brazil), 100 units/ml penicillin, 100 μg/ml streptomycin, 2 mM L-glutamine and 2 mM sodium pyruvate, in a humidified incubator at 5% CO_2 and 37 °C. Neuronal differentiation was induced by addition of 1 μM RA. Formation of EB was induced by culturing P19 cells as cell suspension in bacterial culture dishes coated with 0.2% of final volume with agarose for 48 h at a density of 5×10^5 cells/ml in defined serum-free medium as described previously [20,21]. Completion of neuronal differentiation after 8 days of addition of RA was confirmed by immunostaining against neuron-specific proteins NF-200, β-3-tubulin, and neuron-specific enolase (data not shown). Differentiated P19 cell cultures were kept free from glial cells by treatment with 50 μg/ml cytosine arabinoside on day 6 of differentiation.

2.4. Reverse transcription (RT) and real-time PCR

Total RNA was isolated using the TRIzol reagent (Invitrogen) from embryonic P19 (day 0) and differentiating P19 cells on days 2–8 of differentiation. Contaminating DNA was removed by DNase I (Ambion Inc., Austin, TX) treatment and integrity of the isolated RNA was analyzed on a 2% ethidium bromide-stained agarose gel. Three micrograms of total RNA from days 0 to 8 of differentiation were used in

each case as template for cDNA synthesis in the presence of 50 ng of random primers and 200 units of RevertAid^{TM} H Minus Moloney murine leukemia virus-reverse transcriptase (Fermentas Inc., Hanover, MD) in a total volume of 20 μl for 45 min at 42 °C. PCR reactions were carried out using these cDNAs as templates for amplification to verify gene expression of nAChR and mAChR subtypes. All PCR products were gel-purified, cloned into PGEM T-Easy vectors (Promega, Madison, WI), sequenced and confirmed to be identical to mouse cholinergic receptor cDNA. They were electrophoresed on a 2% agarose gel, visualized by ethidium bromide staining under UV illumination, and verified for their expected size (see Table I of supplemental data). Real-time PCR was performed in order to quantify relative mRNA transcription levels of α_2, α_3, α_4, α_5, α_6, α_7, β_2, β_4 nAChR subunits and M1, M2, M3 mAChR subtypes in embryonic P19 cells and P19 cells undergoing neuronal differentiation. DNA templates were amplified by real time PCR on the 7000 Sequence Detection System (ABI Prism, Applied Biosystems, Foster City, CA, USA) using the Sybr green method [22,23].

Thermal cycling conditions included an initial denaturation step of 95 °C for 10 min and 50 cycles at 95 °C for 15 s and 60 °C for 1 min. Experiments were performed in triplicate for each data point. Nicotinic and muscarinic receptor cDNA abundance was quantified as a relative value compared with an internal reference, β-actin cDNA, whose abundance is believed not to change between the varying experimental conditions [20,24]. Primer sequences used for real time PCR are detailed in Table I of supplemental data.

2.5. Immunoperoxidase and immunofluorescence studies

For immunoperoxidase studies, 5×10^5 cells each from embryonic or differentiating P19 cultures were grown on glass coverslips, fixed in 2% paraformaldehyde for 10 min and dehydrated for 5 min at 37 °C on a preheated platform. For blocking non-specific antibody binding, coverslips were incubated for 2 h with 2% nonfat-milk containing 0.01% saponin and 2% goat or rabbit serum. Then, cells were incubated overnight at 4 °C with primary antibodies at 1/50 dilutions in phosphate-buffered saline (PBS) in the presence of 0.3% Triton X-100 and 5% goat or rabbit serum.

Following washing with PBS, coverslips were incubated for 1 h with biotinylated secondary antibodies at 1/200 dilutions. Unbound antibodies were removed by washing with PBS. Following incubation with avidin–biotin complex for 1 h, specific immunolabeling was revealed by detecting peroxidase activity in the presence of diaminobenzidine and H_2O_2 (Aldrich, Milwaukee, WI). Negative controls were performed by repeating the above procedure in the absence of the respective primary antibody. Images were collected using a Nikon DXM1200F Digital Camera (Nikon, Surrey, UK) coupled to an inverted Axiovert 200 microscope (Zeiss, Jena, Germany), stored into a PC, and analyzed with the Nikon ACT-1 version 2.62 software as described before [25].

2.6. Measurement of free cytosolic calcium concentrations ($[Ca^{2+}]_i$)

Undifferentiated and P19 cells differentiated into neurons following induction with RA were incubated with 4 μM Fluo3-AM in 0.5% Me_2SO and 0.1% of the nonionic surfactant pluronic acid F-127 for 30 min at 37 °C in EM containing (in mM): 140 NaCl, 3 KCl, 1 $MgCl_2$, 2.5 $CaCl_2$, 10 HEPES, pH 7.4, 10 glucose. The osmolarity of all the solutions ranged between 303 and 308 mosmol/l. After loading with Fluo3-AM, the cells were washed with extracellular medium (EM) and incubated for a further 20 min at 37 °C to allow for complete deesterification of the dye. Calcium imaging was performed with a LSM 510 confocal microscope (Zeiss, Jena, Germany), using image sizes of 256 × 256 pixels and acquisition rates of one frame per second. Fluo-3 fluorescence was excited with a 488 nm line of an argon ion laser, and the emitted light was detected using a bandpass filter at 515–530 nm [26]. At the end of each experiment, 5 μM ionophore (4-Br-A23187) followed by 10 mM EGTA were used to determine F_{max} and F_{min} fluorescence values, respectively. The $[Ca^{2+}]_i$ values were calculated from the Fluo3-fluorescence emission using a self-ratio equation as described previously [20] assuming a K_d of 450 nM for Fluo-3 calcium binding [27]. At least 10 cells were analyzed for each data point. For $[Ca^{2+}]_i$ measurement in Ca^{2+}-free medium, cells were pretreated for 5 min with Ca^{2+}-free EM supplemented with 1 mM EGTA prior to cell stimulation. The mean F_{min}/F_{max} ratio was 0.20 ± 0.03 (mean ± S.E.M., $n = 34$) and 0.24 ± 0.03 (mean ± S.E.M., $n = 38$) for short- and long-term measurements, respectively; these values are consistent with those reported for this dye in other systems [28,29]. The average baseline fluorescence normalized to F_{min} was 0.21 ± 0.02 ($n = 42$). Data were calculated as a percentage of F/F_o with F and F_o being Fluo-3 fluorescence emissions of stimulated and unstimulated cells, respectively. No significant effects on basal levels of fluorescence were observed after incubation with any of the antagonists or blockers used, with the exception of $CdCl_2$. Incubation with $CdCl_2$ produced a rather slow but sustained increase in basal fluorescence, which precluded its use in long-term measurements.

Atropine and mecamylamine were employed as specific inhibitors of mAChR and nAChR-induced $[Ca^{2+}]_i$ responses, respectively [30,31]. Pirenzepine (0.1 μM), which at this concentration is a M1 mAChR subtype-specific inhibitor, or 4-diphenylacetoxy-*N*-methylpiperidine methiodide (4-DAMP), a mAChR antagonist with higher specificity for M3 than for other muscarinic subtypes [32,33], were applied together with 3 μM muscarine to elucidate whether M1 and M3 mAChR subtypes were functional in neuronal-differentiated P19 cells. Participation of M2 and M4 subtypes in muscarine-evoked $[Ca^{2+}]_i$ responses was studied in the presence of 10 μM gallamine and 1 μM toxin from the green mamba *D. angusticeps* (MT3), respectively [33–37]. The used inhibitor concentrations elicited maximal effects as increasing their concentrations by a factor of 10 did not result

in any additional inhibition. For characterization of the signal transduction pathway for muscarinic receptor-mediated mobilization of Ca^{2+} from intracellular stores, 5 μM of the PLC inhibitor U-73122 [38] was preincubated with differentiated P19 cells for 5 min prior to $[Ca^{2+}]_i$ measurements. Determination of changes in $[Ca^{2+}]_i$ were performed in the presence of nicotine (100 μM) following preincubation of P19 neurons during 14 min with cyclopiazonic acid (CPA, 10 μM), a sarcoplasmatic/endoplasmatic reticulum Ca^{2+}-ATPase (SERCA) inhibitor [39,40].

Blockers of voltage-operated calcium channels (VOOC), such as $CdCl_2$ [41] nifedipine at 100- and 5-μM concentrations, respectively [41,42], were used to evaluate the participation of these channels in nicotine-evoked increase in $[Ca^{2+}]_i$. These VOOC blockers were preincubated with the cells for 15 min at room temperature in the dark prior to application of nicotine. Preincubation with 40 nM α-bungarotoxin (α-Bgt) was carried out for 30 min before Ca^{2+} measurements in order to evaluate the participation of α_7 nAChR in $[Ca^{2+}]_i$ responses [29].

2.7. Statistical analysis

Data represent the mean ± S.D. of five or more independent experiments (each with two replicates) for RT-PCR and real-time PCR studies. The numbers of experiments to which the data of calcium measurements refer are indicated in respective figure legends. Statistical significances of obtained data were determined using the Student's *t*-test or one-way ANOVA plus *post hoc* Tukey's test, as stated in the figure legends. Values of $p < 0.05$ were considered as statistically significant.

3. Results

3.1. Nicotinic and muscarinic acetylcholine receptor expression during neuronal differentiation of P19 cells

We have detected α_2–α_7 and β_2 and β_4 nAChR as well as M1–M3 mAChR mRNA transcription along P19 cell differentiation by using RT-PCR procedures (Fig. I of supplemental data). Nicotinic β_3 subunit mRNA transcription was below the detection limit of the method, and α_3 and β_2 subunits were only transcribed following induction to neuronal differentiation by RA addition. Gene expression of the three studied M1 and M2 mAChR subtypes was detected throughout the differentiation period. M3 mAChR mRNA was at the limit of detection by RT-PCR in the undifferentiated stage. However, M3 mAChR gene expression subsequently increased following induction of P19 cells to neuronal differentiation.

Real-time PCR revealed that gene expression of $\alpha_2, \alpha_4, \alpha_5, \alpha_6, \alpha_7$ and β_4 nAChR subtypes was already present in embryonic P19 cells, remained then at a lower level during initial and intermediate differentiation stages and increased significantly when differentiating P19 cells became postmitotic and underwent final maturation on days 6–8. Transcription rates for muscarinic receptors (M1–M3) showed an increase in their abundance during neuronal differentiation of P19 cells (Fig. 1).

The presence of nAChR proteins in embryonic P19 cells, P19 progenitor cells on day 4, and P19 cells differentiated into neurons on day 8 was revealed by immunoperoxidase staining using subtype-specific antibodies. Protein expression of all nicotinic subunits besides the β_3 one was detected (Fig. 2).

3.2. Resting $[Ca^{2+}]_i$ levels

Basal calculated $[Ca^{2+}]_i$ levels were 25 ± 10 nM in embryonic cells ($n = 134$) and 70 ± 14 nM in mature neuronal P19 cells ($n = 142$).

3.3. Acetylcholine receptor activity in undifferentiated and neuronal-differentiated P19 cells

Peak values of transient elevations of $[Ca^{2+}]_i$ in embryonic and mature neuronal cell cultures obtained in the presence of a wide range of nicotine and muscarine concentrations were plotted as dose–response curves (Fig. 3A and B). Nicotine- and muscarine-induced effects were dose-dependent and promoted highest elevations of $[Ca^{2+}]_i$ in neuronal-differentiated cells. Muscarine did not induce $[Ca^{2+}]_i$ transient in embryonic P19 cells. The concentration of nicotine necessary for activation of 50% of the maximal receptor activity (EC_{50}) was determined as 33.4 (9.7–115.2) μM for embryonic cells and 52.4 (5.9–465.5) μM (mean values and 95% confidence interval) for neuronal-differentiated cells on day 8. The EC_{50} for muscarinic receptor activation in P19 neurons was 24.3 (5.0–117.2) μM (mean value and 95% confidence interval).

Measurements of acetylcholine (ACh)-induced alterations in $[Ca^{2+}]_i$ provide an independent assay for detective functional cholinergic receptor subtypes in developing P19 neuronal cells. Therefore, we measured $[Ca^{2+}]_i$ responses after application of cholinergic receptor agonists and a selective cholinergic antagonists in undifferentiated and neuronal-differentiated cells. Application of 300 μM ACh evoked a rapid and transient increase in $[Ca^{2+}]_i$ in undifferentiated and neuronal-differentiated cells on day 8. The peak values of $[Ca^{2+}]_i$ in embryonic P19 cells increased in the presence of 300 μM ACh from 32 ± 1 to 78 ± 6 nM ($n = 51$). Stimulation of P19 cells on day 8 of differentiation with 300 μM ACh resulted in increases of $[Ca^{2+}]_i$ from 63 ± 1 to 989 ± 39 nM ($n = 62$) (Fig. 3C).

The relative contributions of mAChRs and nAChRs to the ACh-evoked $[Ca^{2+}]_i$ in undifferentiated and differentiated cells were revealed by calcium imaging in the presence of specific nicotinic and muscarinic receptor antagonists. Co-application of mecamylamine (3 μM), a nAChR antagonist, in combination with 300 μM ACh inhibited the ACh-induced increase in $[Ca^{2+}]_i$ in embryonic P19 cells by 87 ± 10%

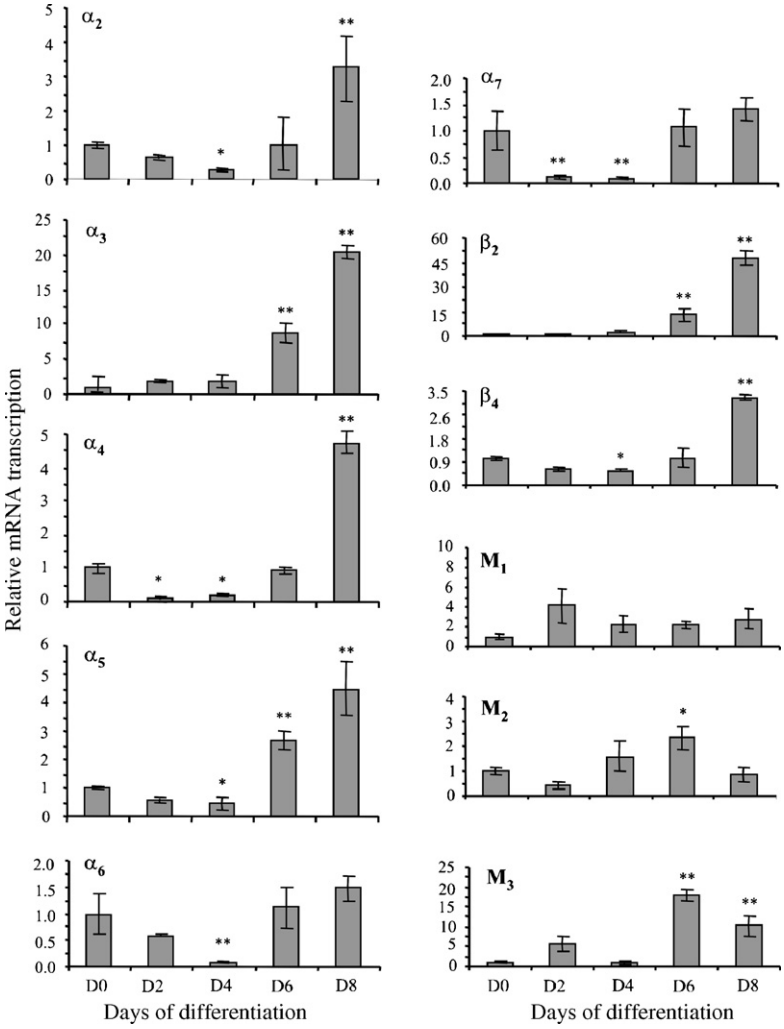

Fig. 1. Quantification of cholinergic receptor mRNA transcription by real-time PCR. Relative gene expression levels of receptors subtypes were corrected with the internal control β-actin. The graphics shows nAChR and mAChR mRNA transcription levels in differentiating cells compared to those in undifferentiated cells which were normalized to one. Cells on day 8 of differentiation were pretreated on day 6 with cytosine arabinoside, in order to avoid contamination of the cell cultures with increasing concentrations of proliferating glial cells. The data shown are mean values ± S.E.M. of at least five independent experiments. $^{*}p < 0.05$, $^{**}p < 0.001$ compared with control data.

($\Delta[Ca^{2+}]_i = 10 \pm 0.3$ nM) compared to the control measurement with ACh alone ($\Delta[Ca^{2+}]_i = 78 \pm 6$ nM). The presence of the mAChR-specific antagonist atropine resulted in non-significant inhibition ($12 \pm 1\%$) of the ACh-induced increase in $[Ca^{2+}]_i$, ($\Delta[Ca^{2+}]_i = 69 \pm 7$ nM), indicating that ACh-induced calcium responses in undifferentiated cells are mainly due to nAChR activation (Fig. 3D). ACh-induced increases in $[Ca^{2+}]_i$ of neuronal-differentiated P19 cells were inhibited by $41 \pm 2\%$ ($\Delta[Ca^{2+}]_i = 586 \pm 23$ nM) or $54 \pm 2\%$ ($\Delta[Ca^{2+}]_i = 456 \pm 24$ nM) in the presence of 3 μM mecamylamine or 1 μM atropine, respectively, compared to control ($\Delta[Ca^{2+}]_i = 993 \pm 70$ nM). Co-application of 3 μM mecamylamine and 1 μM atropine together with acetylcholine resulted in a complete inhibition of the $[Ca^{2+}]_i$ (data not shown). Our data indicate that ACh-induced $[Ca^{2+}]_i$ responses in P19 cells differentiated into neurons are due to nAChR and mAChR activation.

3.4. Sources of Ca^{2+} in P19 neurons mobilized by mAChR and nAChR activation

Relative contributions of extracellular Ca^{2+} and intracellular Ca^{2+} stores to ACh-evoked $[Ca^{2+}]_i$ responses were studied in neuronal-differentiated P19 cells. Preincubation of neurons with Ca^{2+}-free EM containing 1 mM EGTA for 1 min prior to ACh application resulted in inhibition of the $[Ca^{2+}]_i$ response by $44 \pm 4\%$ ($\Delta[Ca^{2+}]_i = 493 \pm 34$ nM) compared to the control experiment ($\Delta[Ca^{2+}]_i = 887 \pm 39$ nM) performed in the presence of extracellular Ca^{2+} (Fig. IIA of supplemental data), indicating involvement of both extracellular and intracellular Ca^{2+} pools in ACh-induced $[Ca^{2+}]_i$ responses. The inhibition of the ACh-induced $[Ca^{2+}]_i$ in P19 neurons in the absence of extracellular Ca^{2+} was abolished after reintroduction of Ca^{2+} into the EM ($\Delta[Ca^{2+}]_i = 955 \pm 35$ nM).

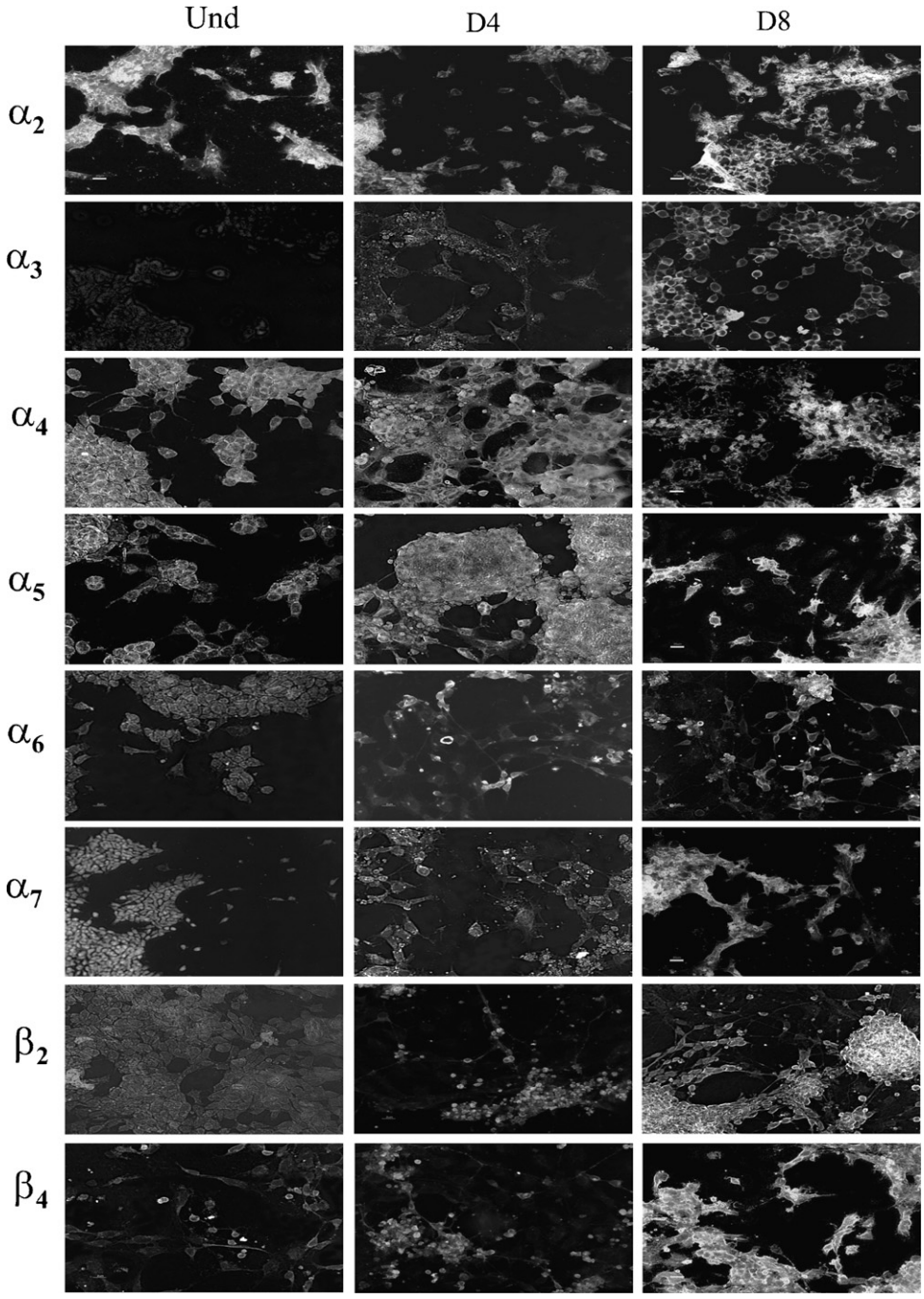

Fig. 2. Detection of expression profiles of neuronal nicotinic acetylcholine receptors during neuronal differentiation of P19 cells by immunoperoxidase staining. Following fixation, cells were incubated with the subunit-specific primary antibody followed by addition of a biotinylated secondary antibody. The reaction was revealed by immunoperoxidase staining. Nicotinic receptor subunit expression was verified in undifferentiated (Und., left panels) and cells on days 4 (D4, middle panels) and 8 (D8, right panels) following induction to neuronal differentiation.

Muscarinic receptor-induced elevations of $[Ca^{2+}]_i$ in the absence of extracellular Ca^{2+} ($\Delta[Ca^{2+}]_i = 492 \pm 34$ nM), obtained by stimulation of differentiated cells by ACh in the presence of 3 μM mecamylamine and 1 mM EGTA ($\Delta[Ca^{2+}]_i = 471 \pm 18$ nM) did not differ from those obtained by ACh alone in Ca^{2+}-containing EM. This result indicates that Ca^{2+} influx from the extracellular medium does not contribute to the mAChR-mediated $[Ca^{2+}]_i$ response in P19 neurons. In the absence of extracellular Ca^{2+}, the ACh-induced $[Ca^{2+}]_i$ response was strongly inhibited by 1 μM atropine ($\Delta[Ca^{2+}]_i = 123 \pm 11$ nM), suggesting the participation of internal Ca^{2+} sources in mAChR-mediated calcium fluxes (Fig. IIB of supplemental data). As expected, influx of Ca^{2+} from the extracellular medium participated to nAChR-

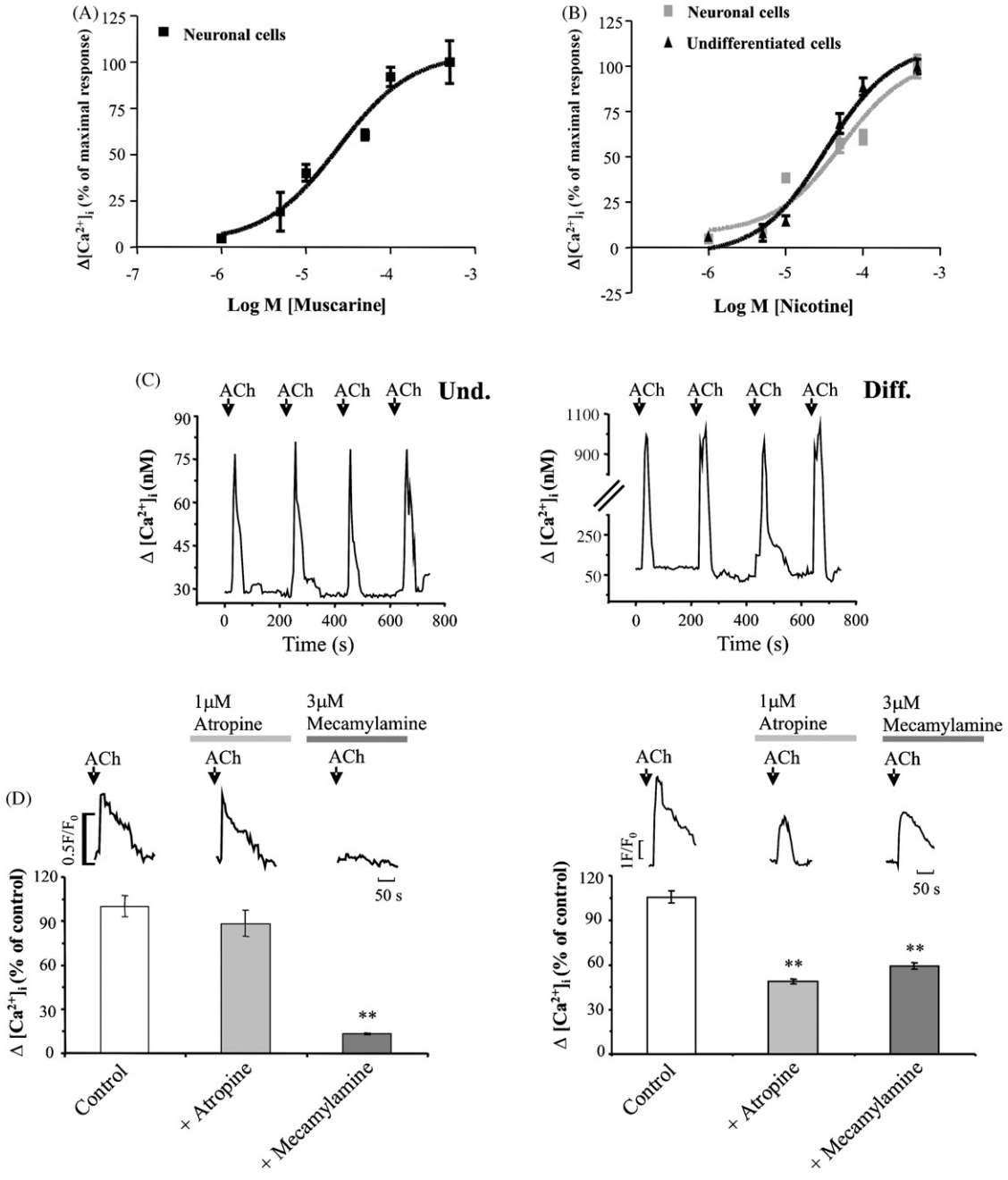

Fig. 3. $[Ca^{2+}]_i$ responses in embryonal P19 cells and neurons on day 8 of differentiation induced by activation of nicotinic and muscarinic acetylcholine receptors. Fluo-3 AM loaded cells were monitored for changes of $[Ca^{2+}]_i$ by calcium imaging using confocal microscopy. (A) Dose–response (EC_{50}) curve of activation of mAChR induced $[Ca^{2+}]_i$ flux in neuronal-differentiated cells by muscarine. Peak fluorescence values of $[Ca^{2+}]_i$ transients were calculated and plotted as percentage of the mean maximum response. (B) Dose–response (EC_{50}) curve of activation of nAChR induced $[Ca^{2+}]_i$ flux in undifferentiated and neuronal-differentiated P19 cells by nicotine. Following stimulation with 300 μM ACh during 30 s the cells were washed with culture medium for 5 min to allow for receptor resensitization. Arrows indicate time points of agonist or agonist and antagonist application. (A) and (B) Data points are mean values ± S.E.M. from 6 to 14 independent experiments. (C) ACh-induced $[Ca^{2+}]_i$ transients in undifferentiated (Und.) and neuronal-differentiated (Diff.) P19 cells. No receptor desensitization was noted under the used experimental conditions, as repeated ACh application did not result in a run down of $[Ca^{2+}]_i$ responses. (D) Left upper panels: embryonic cells were stimulated either by application of ACh alone or of ACh in the presence of 1 μM atropine or 3 μM mecamylamine. Right upper panels: P19 cells differentiated to neurons were stimulated with 300 μM ACh in the absence or presence of ACh receptor inhibitors as indicated above. Lower panels indicate percentage values of $[Ca^{2+}]_i$ increases obtained in the presence of atropine, mecamylamine compared to the control measurement in absence of inhibitors. $[Ca^{2+}]_i$ values in the presence of inhibitors are plotted as percentage of the uninhibited control. All antagonists were preincubated with the cells for at least 10 min and were then co-applied with ACh. The data shown are mean values ± S.E.M. of 8 independent experiments ($n = 8$). The total numbers of cells analyzed in each experiment were 56–81. $^*p < 0.05$, $^{**}p < 0.001$ compared with control data.

mediated elevations in $[Ca^{2+}]_i$. Local perfusion of cells with KCl (75 mM for 30 s) produced a rise in $[Ca^{2+}]_i$ from 29 ± 3 to 215 ± 33 nM ($n = 6$) in undifferentiated and from 68 ± 8 to 715 ± 77 nM ($n = 8$) in neuronal-differentiated cells which was inhibited in the absence of extracellular calcium. Identical results were obtained upon KCl stimulation following washing of the cells for 5 min (Fig. IIA of supplemental data). The effects of mecamylamine and atropine in inhibiting cholinergic receptor activity were abolished after bathing them out ($\Delta[Ca^{2+}]_i = 942 \pm 33$ nM) (data not shown).

$CdCl_2$ (100 μM) in external buffer containing 2.5 mM Ca^{2+} was used in calcium-imaging experiments in order to evaluate the participation of VOOC in the nicotine-induced $[Ca^{2+}]_i$ response in embryonic and neuronal-differentiated P19 cells. The nicotine-evoked increase in $[Ca^{2+}]_i$ was inhibited by more than $87 \pm 20\%$ ($\Delta[Ca^{2+}]_i = 10 \pm 3$ nM) and $54 \pm 3\%$ ($\Delta[Ca^{2+}]_i = 209 \pm 14$ nM) in undifferentiated ($\Delta[Ca^{2+}]_i = 78 \pm 10$ nM) and neuronal-differentiated cells ($\Delta[Ca^{2+}]_i = 456 \pm 70$ nM), respectively (Fig. IIC and D of supplemental data), indicating that VOCC mediate most of the $[Ca^{2+}]_i$ response in undifferentiated and about 50% in neuronal-differentiated cells. The residual nicotine-evoked increase in $[Ca^{2+}]_i$ in the presence of $CdCl_2$ was significantly decreased, by $91 \pm 6\%$ ($\Delta[Ca^{2+}]_i = 7 \pm 0.1$ nM) and $77 \pm 10\%$ ($\Delta[Ca^{2+}]_i = 19 \pm 6$ nM) following co-application of 40 nM α-bungarotoxin (Bgt) and 100 μM $CdCl_2$ together with nicotine in embryonic and neuronal-differentiated cells, respectively (Fig. IIC and D of supplemental data).

The L-type VOCC blocker nifedipine (5 μM) inhibited $68 \pm 7\%$ ($\Delta[Ca^{2+}]_i = 26 \pm 6$ nM) and $38 \pm 5\%$ ($\Delta[Ca^{2+}]_i = 151 \pm 13$ nM) of the nicotine-evoked increase in fluorescence in undifferentiated ($\Delta[Ca^{2+}]_i = 79 \pm 25$ nM) and neuronal-differentiated cells ($\Delta[Ca^{2+}]_i = 456 \pm 68$ nM), respectively. In the presence of nifedipine, α-Bgt produced a statistically significant inhibition of $77 \pm 9\%$ ($\Delta[Ca^{2+}]_i = 19 \pm 6$ nM) and $81 \pm 3\%$ ($\Delta[Ca^{2+}]_i = 88 \pm 9$ nM) of the nicotine-induced $[Ca^{2+}]_i$ in undifferentiated and neuronal-differentiated cells, respectively (Fig. IIC and D of supplemental data). This result suggests that α_7 nAChR are the main mediators of the VOCC-independent increase in intracellular Ca^{2+}, as α-Bgt, at that concentration, inhibits only the α_7 nAChR subtype [29]. Furthermore, nAChR-mediated elevations of $[Ca^{2+}]_i$ in embryonic P19 cells were not significatively different in the presence of nifedipine alone and nifedipine plus α-Bgt, indicating that nicotine-activated calcium flux depends on VOOC activation. However, in neuronal-differentiated P19 cells about 40% of the nicotine-induced $[Ca^{2+}]_i$ response is mediated by VOCC and the remaining response is due to the mobilization of internal Ca^{2+} pools and by calcium-influx through nAChR channels themselves.

Pirenzepine (0.1 μM), gallamine (10 μM), 4-DAMP (0.1 μM) and MT3 (1 μM), which at these concentrations are specific antagonists of M1 [33], M2 [34,35] M3, [33] and M4 [36,37] mAChRs, respectively, were co-applied together with 300 μM muscarine, in order to elucidate the contribution of each subtype to the mAChR-mediated $[Ca^{2+}]_i$ response in differentiated P19 cells. Among these inhibitors, 4-DAMP is a less selective antagonist with an inhibition profile of M3 > M1 ≫ M5 subtypes [33,34]. Treatment of neurons with pirenzepine resulted in an inhibition of the muscarine-induced $[Ca^{2+}]_i$ response by $12 \pm 1\%$ ($\Delta[Ca^{2+}]_i = 492 \pm 22$ nM) compared to the control experiment ($\Delta[Ca^{2+}]_i = 560 \pm 23$ nM) in the absence of the inhibitor. A higher reduction of mAChR-evoked $[Ca^{2+}]_i$ response by $26 \pm 2\%$ was observed in the presence of 4-DAMP ($\Delta[Ca^{2+}]_i = 415 \pm 12$ nM), which at 0.1 mM concentration preferentially inhibits the M3 subtype. The presence of gallamine as a specific antagonist of the M2 subtype also led to an inhibition of the muscarine-induced calcium flux by $30 \pm 1\%$ ($\Delta[Ca^{2+}]_i = 390 \pm 17$ nM). The M4 subtype-specific inhibitor MT3 caused the smallest inhibition ($9 \pm 1\%$) in neuronal-differentiated cells which was not statistically significant than compared to mAChR-mediated elevations of $[Ca^{2+}]_i$ in control experiments ($\Delta[Ca^{2+}]_i = 511 \pm 28$ nM). Co-application of all four inhibitors resulted in inhibition of the muscarine-induced calcium response by $78 \pm 4\%$ ($\Delta[Ca^{2+}]_i = 122 \pm 6$ nM) (Fig. 4A). The total observed inhibition in the presence of all four inhibitors was the sum of the effects found in the presence of each inhibitor alone. The inhibition of the muscarinic receptor response caused by the presence of a cocktail of pirenzepine, gallamine, 4-DAMP and MT3 was reversible as receptor responses recovered following washing out of the inhibitors ($\Delta[Ca^{2+}]_i = 571 \pm 35$ nM). The remaining $[Ca^{2+}]_i$ response in the presence of the four inhibitors may be due to M5 mAChR activity which was not affected by either one of these mAChR antagonists.

Our data indicate that around 60% of muscarinic receptor-induced elevation in $[Ca^{2+}]_i$ in neuronal-differentiated P19 cells is due to activation of M1, M3, and M5 subtypes, which can simultaneously activate multiple signaling pathways [43]. These G_q-coupled receptors exert their signal transduction by activating phospholipase C (PLC). Preincubation of P19 neurons with U-73343 (5 μM), as a specific inhibitor of PLC pathway, resulted in a significant inhibition, $60 \pm 2\%$ ($\Delta[Ca^{2+}]_i = 224 \pm 5$ nM), of the $[Ca^{2+}]_i$ response induced by muscarine ($\Delta[Ca^{2+}]_i = 561 \pm 21$ nM), confirming the participation of PLC in mAChR-induced $[Ca^{2+}]_i$ mobilization (Fig. 4B). The percentage of inhibition of muscarine-induced elevation in $[Ca^{2+}]_i$ in the presence of blockage of PLC activity was similar to that observed when inhibitors for M1, M3 and M5 were co-applied ($60 \pm 6\%$) (Fig. 4A). Following washing U-73122 out the response to muscarine was similar to that observed in control experiments ($\Delta[Ca^{2+}]_i = 517 \pm 26$ nM) (data not shown). Further control experiments performed following preincubation of P19 neurons with the biologically inactive analog U-73122 did not affect muscarine-induced $[Ca^{2+}]_i$ responses ($\Delta[Ca^{2+}]_i = 515 \pm 16$ nM). These results indicate that, M1,

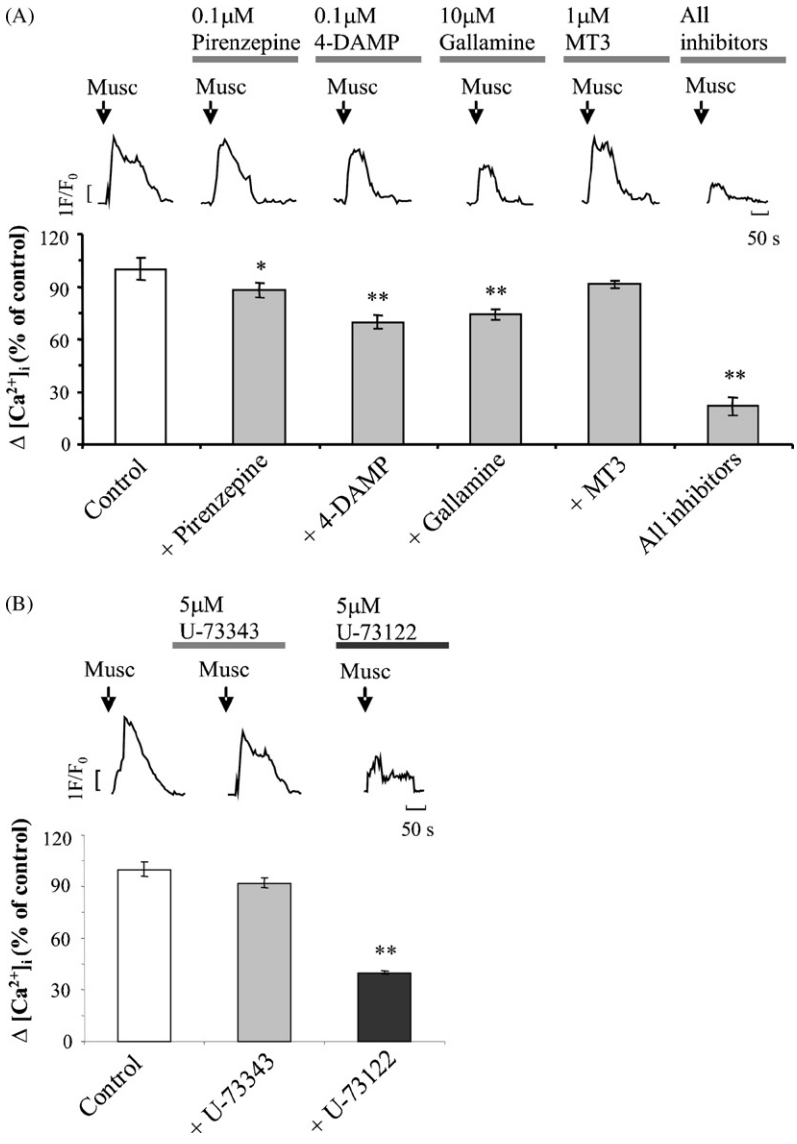

Fig. 4. Characterization of muscarinic acetylcholine receptor (mAChR) induced elevation of $[Ca^{2+}]_i$ in P19 neurons. (A) The upper panel shows traces of alterations of $[Ca^{2+}]_i$ of P19 cells on day 8 of differentiation following stimulation with 300 μM of muscarine (Musc) alone or together with 0.1 μM pirenzipine ($n = 8$), 0.1 μM 4-DAMP ($n = 8$), 10 μM galamine ($n = 8$), or 1 μM MT3 ($n = 8$) which are specific inhibitors of M1, M3, M2 and M4 mAChR subtypes, respectively. None of the used inhibitors are antagonists of M5 mAChR activity. The remaining alteration of $[Ca^{2+}]_i$ following stimulation by muscarine in the presence of all four inhibitor is believed to be due to activation of the M5 subtype ($n = 4$). Lower panels: average $[Ca^{2+}]_i$ values in the presence of the respective inhibitors were plotted as percentage of control measurements performed in the absence of inhibitors. (B) The upper panel shows traces of $[Ca^{2+}]_i$ transients obtained following stimulation with muscarine alone or with muscarine in the presence of 5 μM of PLC inhibitor U-73122 and its biologically inactive analog U-73343. In the lower panels, $[Ca^{2+}]_i$ values obtained in the presence of muscarine and U-73122 ($n = 4$) or U-73343 ($n = 8$) were plotted as percentage of the control measurements in the absence of inhibitors ($n = 8$). The total number of cells analyzed in each experiment was 56–76. Data are presented as mean values ± S.E.M.; $*p < 0.05$, $**p < 0.001$ compared with control data.

M3, and M5 mAChRs in P19 cells differentiated into neurons couple to PLC, thereby stimulating the production of inositol triphosphate (IP_3) followed by release of Ca^{2+} from intracellular stores.

We have also determined the concentration of muscarinic receptor subtype-selective antagonists necessary to inhibit 50% of the muscarine-induced $[Ca^{2+}]_i$ response (IC_{50}) in these cells. The effect of 300 μM muscarine in inducing elevations in $[Ca^{2+}]_i$ in neuronal-differentiated cells was partially and dose-dependently blocked by pirenzepine, gallamine, and 4-DAMP (Fig. III of supplemental data). Respective potencies of the antagonists determined as pK_i values with confidence intervals were 5.56 (7.3–3.8), 6.46 (8.7–4.3) and 6.03 (6.66–5.41) for 4-DAMP, gallamine and pirenzepine, respectively. The results of the IC_{50} determination indicate that the effect of muscarine in inducing $[Ca^{2+}]_i$ transients was predominately mediated by a M3-like receptor subtype. Antagonist concentrations higher than those used in these experiments unspecifically inhibit other muscarinic subtypes.

3.5. Dependence of nAChR-induced $[Ca^{2+}]_i$ responses on the presence of extracellular Ca^{2+} and Ca^{2+} release from internal Ca^{2+} stores

Caffeine in milimolar concentrations acts as inhibitor of intracellular receptors for IP_3, as well as activator of ryanodine receptors [44], thereby depleting intracellular ryanodine-sensitive Ca^{2+} stores [45]. In contrast, micromolar concentrations of ryanodine inhibit caffeine-induced Ca^{2+} release from intracellular Ca^{2+} stores. Caffeine (10 mM)-induced Ca^{2+} mobilization ($\Delta[Ca^{2+}]_i = 1012 \pm 41$ nM) in P19 neurons was blocked by 10 μM ryanodine ($\Delta[Ca^{2+}]_i = 136 \pm 38$ nM), indicating the presence of ryanodine-sensitive intracellular Ca^{2+} stores (Fig. 5A). These Ca^{2+} stores are responsible for Ca^{2+}-induced Ca^{2+} release CICR, which has already been known to participate in nAChR-induced elevation of $[Ca^{2+}]_i$.

Our data provide further evidence for participation of ryanodine-sensitive Ca^{2+} stores in the nAChR-mediated $[Ca^{2+}]_i$ response (Fig. 5B). Co-application of 300 μM ACh, 1 μM atropine and 10 μM ryanodine to differentiated P19 neurons resulted in larger inhibition, ($72 \pm 2\%$ ($\Delta[Ca^{2+}]_i = 249 \pm 25$ nM), than that obtained in the presence of ACh and atropine alone, ($45 \pm 5\%$

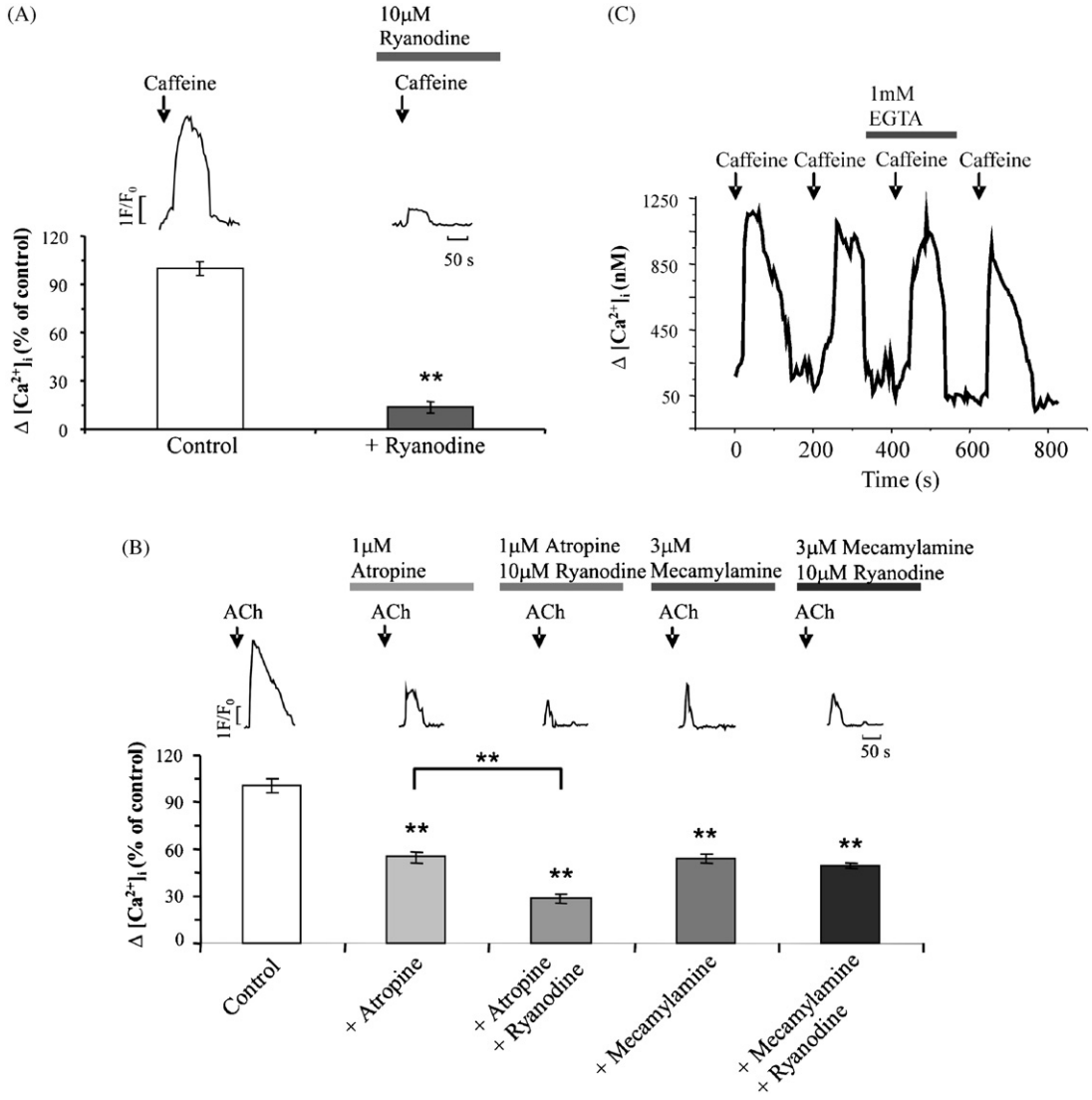

Fig. 5. Dependence of nicotinic receptor activation in P19 neurons on intracellular ryanodine-sensitive calcium stores. Upper panel: (A) Alterations of $[Ca^{2+}]_i$ in P19 neurons on day 8 of differentiation following application of 10 mM caffeine (during 30 s of application) with or without preincubation of cells for 30 min with 10 μM ryanodine. (B) Representative traces of $[Ca^{2+}]_i$ responses after application of 300 μM ACh in the absence or presence of 1 μM atropine, or after co-application of 300 μM ACh with 1 μM atropine or 3 μM mecamylamine following preincubation of cells for 30 min with 10 μM ryanodine. Lower panels: mean $[Ca^{2+}]_i$ values ± S.E.M. obtained in the presence of inhibitors were plotted as percentages of the control value obtained in the absence of inhibitors. The data shown were obtained from 4 (A) and 8 (B) independent experiments, respectively. (C) Caffeine-induced $[Ca^{2+}]_i$ responses of neuronal-differentiated cells. Neuronal cells were stimulated with caffeine (10 mM) in the presence or absence of extracellular Ca^{2+} (EGTA 1 mM). Typical $[Ca^{2+}]_i$ traces were from four distinct experiments. For each experiment 28–64 cells were used. The data are presented as mean values ± S.E.M.; $^{**}p < 0.001$ compared with control data.

Table 1
Inhibition of nicotine-induced $[Ca^{2+}]_i$ responses following preincubation with cyclopiazonic acid (CPA)

Time (min)	$\Delta[Ca^{2+}]_i$ (nM)		Relative $\Delta[Ca^{2+}]_i$	
	Control	CPA (10 μM)	Control	CPA (10 μM)
0	467 ± 15	466 ± 16	1.00 ± 0.032	1.00 ± 0.034
7.5	498 ± 15	503 ± 21	1.06 ± 0.033	1.08 ± 0.044
10.5	457 ± 14	403 ± 24	0.98 ± 0.029	0.86 ± 0.051
13.8	450 ± 13	338 ± 24	0.96 ± 0.028	0.72 ± 0.050
16.8	440 ± 15	311 ± 18	0.94 ± 0.033	0.66 ± 0.038
19.5	410 ± 25	234 ± 11	0.88 ± 0.054	0.50 ± 0.023

Relative $\Delta[Ca^{2+}]_i$ = increases in $[Ca^{2+}]_i$ compared to those obtained in the presence of 100 μM nicotine at time point 0.

($\Delta[Ca^{2+}]_i = 489 \pm 35$ nM), when compared to control experiments in the absence of atropine and ryanodine ($\Delta[Ca^{2+}]_i = 887 \pm 39$ nM). No further increase in inhibition was observed when 300 μM ACh, 3 μM mecamylamine and 10 μM ryanodine were co-applied to P19 neurons ($\Delta[Ca^{2+}]_i = 440 \pm 13$ nM) in comparison to the ACh-evoked $[Ca^{2+}]_i$ response in the presence of 3 μM mecamylamine alone ($\Delta[Ca^{2+}]_i = 474 \pm 27$ nM). These data indicate that nAChR-induced Ca^{2+} fluxes involve CICR mediated by ryanodine receptors. The inhibitory effect caused by ryanodine was reversible following excessive washing. Peak values in $[Ca^{2+}]_i$ response induced by application of 300 μM ACh in the presence ($\Delta[Ca^{2+}]_i = 465 \pm 41$ nM) or absence ($\Delta[Ca^{2+}]_i = 878 \pm 45$ nM) of atropine and in the presence ($\Delta[Ca^{2+}]_i = 467 \pm 21$ nM) or absence of mecamylamine ($\Delta[Ca^{2+}]_i = 894 \pm 39$ nM) recovered to those that had been measured without ryanodine treatment. In contrast, CICR mediated by activation of ryanodine receptors did not participate in mAChR-evoked increase of $[Ca^{2+}]_i$ (Fig. 5B).

Nicotine (100 μM)-induced Ca^{2+} fluxes were monitored at different time points following preincubation with 10 μM cyclopiazonic acid (CPA) as an inhibitor of Ca^{2+}-ATPase of the endoplasmatic and sarcoplasmatic reticulum that depletes ryanodine- and IP_3-sensitive calcium stores [44,46]. Pretreatment of neurons with CPA caused a time-dependent decrease of nicotine-induced Ca^{2+} fluxes (50 ± 2%), which was not observed in untreated control cells (Fig. 6A). The continuous decline in the amplitudes of nicotine-induced $[Ca^{2+}]_i$ response indicates slow depletion of intracellular Ca^{2+} stores due to continuous Ca^{2+} release in the presence of CPA. Table 1 shows the values of $\Delta[Ca^{2+}]_i$ and the relative $\Delta[Ca^{2+}]_i$ induced by nicotine at various time points in the absence or presence of CPA treatment.

The percentage of participation of IP_3- and ryanodine-sensitive intracellular calcium stores in neuronal-differentiated cells was verified by calcium-imaging experiments in the presence of CPA and caffeine. Activation of IP_3 receptors in neurons leads to the mobilization of Ca^{2+} from internal Ca^{2+} stores [46]. The $[Ca^{2+}]_i$ response induced by 10 μM CPA during 20 s of application on neuronal-differentiated cells was determined to evaluate the involvement of IP_3-sensitive stores in releasing Ca^{2+}. CPA-application promoted a $[Ca^{2+}]_i$ transient of 298 ± 32 nM ($n = 41$) (Fig. 6B). No statistically relevant differences between CPA-induced $[Ca^{2+}]_i$ elevations were observed, when the cells had been washed for at least 10 min between individual CPA-applications (data not shown).

In summary, CICR via ryanodine-sensitive intracellular Ca^{2+} stores as well as Ca^{2+} influx from the extracellular medium contribute to ACh-evoked elevations of $[Ca^{2+}]_i$ in neuronal-differentiated P19 cells.

4. Discussion

The presence of α_3, α_4, β_2 nAChR subunits and M1, M2, M3, M5 mAChR subtypes during neuronal differentiation of P19 cells has already been reported by Cauley et al. [12] and Parnas et al. [18], respectively. Expression of the M3 subtype and muscarinic receptor activity were significantly augmented in P19 cells differentiated into neurons when compared to undifferentiated cells [18,20]. However, nAChR gene expression and functionality in embryonic P19 cells and differential gene expression and activity of cholinergic receptor subtypes have not been yet studied along the course of neuronal differentiation of this cell line.

In this study, we bring evidence that functional nicotinic receptor channels are already present in the embryonic P19 cells as well as in neural progenitor stages following stimulation to neuronal differentiation by RA. Gene and protein expression of nicotinic receptor subunits, such as α_2–α_7, β_2 and β_4, were detected in these cells throughout neuronal differentiation as evidenced by real-time PCR and immunohistochemistry procedures. In accordance with our findings, nAChR gene expression has already been detected in embryonic tissues and cells [4]. Transcription of nAChR-subunit specific mRNAs has also been reported from embryonic cortex of rodents at the 12th day of embryonic development [4], and nAChR activity has been detected in BLC6 embryonic cells, which have the ability to differentiate into cells with characteristics of skeletal muscle [47]. The expression of functional nAChR in embryonic cell lines capable to differentiate into cell types of all three germinative layers raises the question about the function of these receptors in embryonic and progenitor cells during initial brain development.

Gene expression of α_2, α_4, α_5, α_6, α_7 and β_4 subunits was present in undifferentiated P19 cells and then down-regulated in progenitor stages when cells had already been committed to neuronal differentiation. The initial upregulation of expression of these subunits may point to a participation of nAChRs in early proliferation events and the onset of neuronal differentiation. We have shown that the main ACh-induced response in undifferentiated cells was due to nAChR activation. In agreement with our data obtained during *in vitro* differentiation, Atluri et al. [9] reported that functional nAChRs were present as early as embryonic day 10 in mouse cerebral cortex, when the cortex yet consisted of dividing stem and progenitor cells. Choline present in plasma

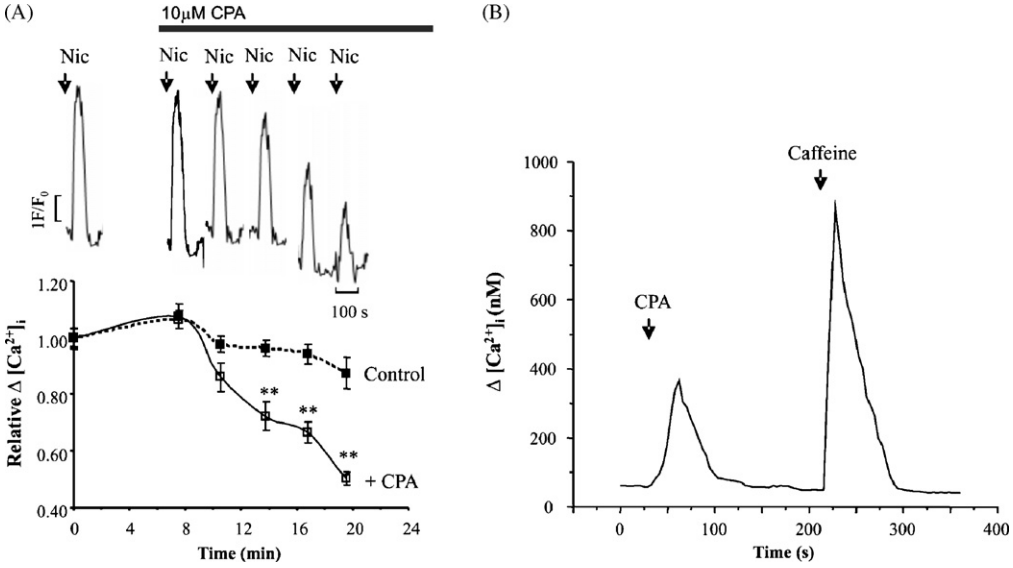

Fig. 6. Nicotinic acetylcholine receptor activation in P19 neurons results in liberation of Ca^{2+} from intracellular calcium stores. (A) Upper panel: traces show the time-dependent inhibition of nicotine (100 μM, Nic)-induced $[Ca^{2+}]_i$ responses by 10 μM cyclopiazonic acid (CPA) present during 14 min. Lower panel: nicotine-induced alterations of $[Ca^{2+}]_i$ obtained in the presence of CPA were normalized to those obtained in control experiments at time point zero. For each data point obtained by stimulation with nicotine in the presence of CPA ($n = 6$) (open boxes), control measurements ($n = 6$) were performed in the absence of CPA (filled boxes). With exception of the first and second data point obtained at 8 min and 10.5 min of preincubation of cells with CPA, all following data points demonstrated significant inhibition of nicotine-induced $[Ca^{2+}]_i$ response in the presence of CPA. Data are presented as mean values ± S.E.M.; $^{**}p < 0.001$ compared with control data. (B) Amplitudes of CPA- and caffeine-induced $[Ca^{2+}]_i$ response in neuronal-differentiated cells. Cells were stimulated sequentially with CPA (10 μM) and caffeine (10 mM). $[Ca^{2+}]_i$ traces shown are representative data from five independent experiments. For each experiment 40–45 cells were used.

membranes could act as an endogenous activator of nAChR activity, taking into account that it possesses high affinity to α_7 homomeric receptors, which are expressed by almost all cells of an undifferentiated P19 population. Choline has been shown to elicit $[Ca^{2+}]_i$ responses in chromaffin cells [48]. Changes in choline concentrations have also been shown to affect postnatal cerebral development in rats [49].

In agreements with already published studies [9,50], 300 μM ACh evoked maximal cholinergic receptor-induced increases in $[Ca^{2+}]_i$. We have also demonstrated that cholinergic receptor-mediated Ca^{2+} fluxes in P19 neurons result from influx of Ca^{2+} from the extracellular medium as well as from mobilization of intracellular Ca^{2+} stores. In embryonic cells, ACh-induced $[Ca^{2+}]_i$ elevations resulted mainly from nAChR activation, as determined by $[Ca^{2+}]_i$ measurements in the presence of atropine and mecamylamine as specific inhibitors of mAChRs and nAChRs, respectively. In neuronal-differentiated P19 cells, ACh-induced $[Ca^{2+}]_i$ responses resulted from almost equal contributions of mAChRs and nAChRs. ACh-induced elevations of $[Ca^{2+}]_i$ in P19 cells terminating their differentiation process ranged around 1 μM as compared to ACh-evoked $[Ca^{2+}]_i$ responses of 100 nM in embryonic P19 cells. The higher amplitudes of changes of $[Ca^{2+}]_i$ in P19 neurons compared to embryonal cells following ACh application may not be only due to a higher fraction of active receptors in differentiated cells, but also to the increased expression of VOOC which are activated following membrane depolarization caused by the initial ACh-induced calcium flux and contributing to the acetylcholine receptor response [51]. Neuronal nAChRs, and particularly homomeric nicotinic receptors formed by the α_7 subtype, exhibit high relative permeability to Ca^{2+} [52,53]. Thus, opening of the nAChR channel can lead to a direct increase in cytoplasmic Ca^{2+} concentration, whilst Na^+ influx can cause neuronal depolarization and activation of VOCC and subsequent amplification of Ca^{2+} transients [54,55].

The intracellular ryanodine-sensitive Ca^{2+} store, a CICR channel, whose activity is regulated by cytosolic Ca^{2+} concentrations, participates to the modulation and amplification of Ca^{2+} signals in various neuronal cells (reviewed in [56]). We have shown that activation of ryanodine-sensitive Ca^{2+} stores are responsible for approximately 50% of the nAChR-mediated $[Ca^{2+}]_i$ responses. More evidence for the presence of CICR in P19 neuronal cells was brought by the observation that caffeine-induced elevations in $[Ca^{2+}]_i$ were blocked in the presence of ryanodine, a specific inhibitor of CICR channels. Participation of CICR channels in regulation of $[Ca^{2+}]_i$ has already been suggested in developing rat motor neurons [46].

Ryanodine-sensitive Ca^{2+} stores (CICR-channels) are apparently not involved in the nAChR-mediated $[Ca^{2+}]_i$ response in undifferentiated P19 cells. These results may be explained by the absence of such stores in embryonic cells and is in agreement with *in vivo* studies that have shown that ryanodine receptors are only expressed in the developing nervous system following the onset to neuronal

differentiation [57]. Further support for this hypothesis was obtained by the observation that in the presence of $CdCl_2$ and nifedipine as inhibitors of VOOC-activity nicotine-induced $[Ca^{2+}]_i$ responses in embryonic cells were almost completely inhibited. However, these inhibitors only promoted an approximate 50%-inhibition the nicotine-induced $[Ca^{2+}]_i$ response in neuronal-differentiated P19 cells, suggesting that CICR-channels participate in the remaining 50% of the nicotine-evoked $[Ca^{2+}]_i$ increase.

The inhibition of nicotine-induced $[Ca^{2+}]_i$ responses following preincubation of P19 neurons with CPA as an inhibitor of endoplasmatic Ca^{2+}-ATPase in order to deplete IP_3- and ryanodine-sensitive Ca^{2+} stores [44,46] again indicated intracellular Ca^{2+} mobilization, such as CICR, as a part of the nAChR-mediated $[Ca^{2+}]_i$ response. In agreement with our results, Dajas-Bailador et al. [58] demonstrated that activation of nAChRs in SH-SY5Y neuroblastoma cells involved VOOC and release of Ca^{2+} from intracellular stores. Similar results were obtained for hippocampal astrocytes [29].

The treatment of cells with CPA alone leads to a transient rise of cytosolic Ca^{2+} due to the leakage of Ca^{2+} from CPA-sensitive stores. In most cell types studied, this Ca^{2+} leakage can be rather variable, but it usually leads to a complete depletion of the endoplasmatic Ca^{2+} stores within a few minutes [59]. Ca^{2+} leakage from intracellular stores was shown to be inhibited in the presence of Ni^{2+} and is presumably mediated by a special channel in the membrane of the endoplasmatic reticulum [60]. In the absence of extracellular Ca^{2+}, this transient Ca^{2+} rise may provide an estimative quantification of the concentration of Ca^{2+} accumulated in CPA-sensitive stores. In cultured rat dorsal root ganglia neurons, concentrations of up to 270 μM Ca^{2+} were identified in endoplasmic reticular stores, by using fluorophores with low-affinity for Ca^{2+} [61]. Caffeine-sensitive calcium stores (CICR) have been described in many vertebrate neurons *in situ* and *in vitro* (reviewed in [62]). However, more than one mechanism exists by which nAChR activation results in transient elevations of $[Ca^{2+}]_i$. For instance, Foucart et al. [63] demonstrated that nAChR activation in rat sympathetic neurons did not depend on intracellular Ca^{2+} stores. In this regard, our study has demonstrated that sources used for nAChR-induced $[Ca^{2+}]_i$ responses change during neuronal differentiation of P19 cells. In undifferentiated P19 cells extracellular Ca^{2+} was the principal source used by the nicotinic component. In P19 cells differentiated into neurons, intracellular Ca^{2+} stores were the main source for nAChR- as well as for mAChR-mediated Ca^{2+} fluxes.

The participation of the muscarinic component in the ACh-induced calcium flux was monitored in the presence of the nAChR-specific inhibitor mecamylamine. Muscarinic receptor-induced elevations of $[Ca^{2+}]_i$ remained in the absence of extracellular Ca^{2+}, suggesting the mAChR-mediated $[Ca^{2+}]_i$ response principally involves intracellular Ca^{2+} stores. In the presence of the PLC inhibitor, U-73122, most of the mAChR-induced $[Ca^{2+}]_i$ was abolished, again indicating that mAChR activation enhances PLC activity, IP_3-formation, and Ca^{2+} release from IP_3-sensitive stores. We have investigated the participation of different mAChR subtypes in the muscarine-induced Ca^{2+} mobilization. The $[Ca^{2+}]_i$ measurements in the presence of subtype-specific inhibitors indicated activities of M1, M2, M3, and M5-subtypes in neuronal-differentiated P19 cells, which are in accordance with previously published data [18,20]. The involvement of mAChRs in neuronal differentiation has previously been studied (reviewed in [16]). For instance, differentiation of neural stem cells depended on the activity of M2 receptor subtypes, as this differentiation was blocked in the presence of the muscarinic antagonist atropine [64]. Inhibition of kinin-B2 receptors during the final neuronal differentiation of P19 cells resulted in a subsequent decrease of M1, M2, and M3 mAChR gene expression and activity, pointing again at a crucial function of muscarinic receptor function in later neuronal differentiation [20].

Taken together, this work contributes to a better understanding of the mechanism of cholinergic receptor activation during early embryogenesis *in vitro*. *In vitro* neuronal differentiation resembles conditions of initial neuroectodermal differentiation [65]. At the onset of differentiation, mostly α_7-type nAChRs, which are highly permeable for Ca^{2+}, contributed to $[Ca^{2+}]_i$ transients, necessary for triggering neurogenesis. The most expressed nAChR in undifferentiated P19 cells was formed by α_7 subunits, followed by $\alpha_2\beta_4$ nAChRs (data not shown). Some other nAChR types such as $\alpha_3\beta_4$ and $\alpha_4\beta_2$ may not be formed during differentiation since expression of α_3 and β_2 subunits was low (Figs. 1 and 2). Following commitment to a neuronal phenotype and undergoing final differentiation, nicotinic and muscarinic receptor types were functional. Ca^{2+} spikes reaching micromolar concentrations were induced by combined Ca^{2+} fluxes from the extracellular medium and intracellular Ca^{2+} stores. These high concentrations in $[Ca^{2+}]_i$ may be necessary for final synaptogenesis, maintaining synaptogenesis and induction of neurotransmitter release.

Conflict of interest statement

None.

Acknowledgments

H.U. and L.R.G.B. are grateful for grants from FAPESP (Fundação de Amparo à Pesquisa do Estado de São Paulo) and CNPq (Conselho Nacional de Desenvolvimento Científico e Tecnológico), Brazil. R.R's and K.N.G.'s Ph.D. theses were or are supported, respectively, by CAPES (Coordenação de Aperfeiçoamento de Pessoal de Nível Superior), Brazil. The Center for Applied Toxinology (CAT-CEPID), Butantan Institute, São Paulo, Brazil, is acknowledged for performing DNA sequencing. We also wish to thank Adilson da Silva Alves, Departamento de Fisiologia e Biofísica, Insti-

tuto de Ciências Biomédicas, Universidade de São Paulo, São Paulo, Brazil, for helping us with immunohistochemistry procedures.

Appendix A. Supplementary data

Supplementary data associated with this article can be found, in the online version, at doi:10.1016/j.ceca.2007.04.007.

References

[1] X. Du, L. Iacovitti, Synergy between growth factors and transmitters required for catecholamine differentiation in brain neurons, J. Neurosci. 15 (1995) 5420–5427.
[2] J. Zhou, H.F. Bradford, G.M. Stern, Induction of dopaminergic neurotransmitter phenotype in rat embryonic cerebrocortex by the synergistic action of neurotrophins and dopamine, Eur. J. Neurosci. 8 (1996) 2328–2339.
[3] S. Wonnacott, N. Sidhpura, D.J. Balfour, Nicotine: from molecular mechanisms to behaviour, Curr. Opin. Pharmacol. 5 (2005) 53–59.
[4] M. Zoli, N. Le Novere, J.A. Hill Jr., J.P. Changeux, Developmental regulation of nicotinic ACh receptor subunit mRNAs in the rat central and peripheral nervous systems, J. Neurosci. 15 (1995) 1912–1939.
[5] P. Brehm, L. Henderson, Regulation of acetylcholine receptor channel function during development of skeletal muscle, Dev. Biol. 129 (1988) 1–11.
[6] H.R. Brenner, V. Witzemann, B. Sakmann, Imprinting of acetylcholine receptor messenger RNA accumulation in mammalian neuromuscular synapses, Nature 344 (1990) 544–547.
[7] A.C. Missias, G.C. Chu, B.J. Klocke, J.R. Sanes, J.P. Merlie, Maturation of the acetylcholine receptor in skeletal muscle: regulation of the AChR gamma-to-epsilon switch, Dev. Biol. 179 (1996) 223–238.
[8] J.R. Sanes, J.W. Lichtman, Induction, assembly, maturation and maintenance of a postsynaptic apparatus, Nat. Rev. Neurosci. 2 (2001) 791–805.
[9] P. Atluri, M.W. Fleck, Q. Shen, et al., Functional nicotinic acetylcholine receptor expression in stem and progenitor cells of the early embryonic mouse cerebral cortex, Dev. Biol. 240 (2001) 143–156.
[10] I. Aubert, D. Cecyre, S. Gauthier, R. Quirion, Comparative ontogenetic profile of cholinergic markers, including nicotinic and muscarinic receptors, in the rat brain, J. Comp. Neurol. 369 (1996) 31–55.
[11] J.A. Court, S. Lloyd, M. Johnson, et al., Nicotinic and muscarinic cholinergic receptor binding in the human hippocampal formation during development and aging, Brain Res. Dev. Brain Res. 101 (1997) 93–105.
[12] K. Cauley, M. Marks, L.C. Gahring, S.W. Rogers, Nicotinic receptor subunits alpha 3, alpha 4, and beta 2 and high affinity nicotine binding sites are expressed by P19 embryonal cells, J. Neurobiol. 30 (1996) 303–314.
[13] L.A. Volpicelli, A.I. Levey, Muscarinic acetylcholine receptor subtypes in cerebral cortex and hippocampus, Prog. Brain Res. 145 (2004) 59–66.
[14] W. Ma, D. Maric, B.S. Li, et al., Acetylcholine stimulates cortical precursor cell proliferation in vitro via muscarinic receptor activation and MAP kinase phosphorylation, Eur. J. Neurosci. 12 (2000) 1227–1240.
[15] S. Biagioni, A.M. Tata, A. De Jaco, G. Augusti-Tocco, Acetylcholine synthesis and neuron differentiation, Int. J. Dev. Biol. 44 (2000) 689–697.
[16] H. Ulrich, P. Majumder, Neurotransmitter receptor expression and activity during neuronal differentiation of embryonal carcinoma and stem cells: from basic research towards clinical applications, Cell Prolif. 39 (2006) 281–300.
[17] D. Parnas, M. Linial, Cholinergic properties of neurons differentiated from an embryonal carcinoma cell-line (P19), Int. J. Dev. Neurosci. 13 (1995) 767–781.
[18] D. Parnas, E. Heldman, L. Branski, N. Feinstein, M. Linial, Expression and localization of muscarinic receptors in P19-derived neurons, J. Mol. Neurosci. 10 (1998) 17–29.
[19] S. Ben-Ari, D. Toiber, A.S. Sas, H. Soreq, Y. Ben-Shaul, Modulated splicing-associated gene expression in P19 cells expressing distinct acetylcholinesterase splice variants, J. Neurochem. 97 (2006) 24–34.
[20] A.H. Martins, R.R. Resende, P. Majumder, et al., Neuronal differentiation of P19 embryonal carcinoma cells modulates kinin B2 receptor gene expression and function, J. Biol. Chem. 280 (2005) 19576–19586.
[21] R.R. Resende, P. Majumder, K.N. Gomes, L.R. Britto, H. Ulrich H, P19 embryonal carcinoma cells as *in vitro* model for studying purinergic receptor expression and modulation of *N*-methyl-D-aspartate–glutamate and acetylcholine receptors during neuronal differentiation, Neuroscience 146 (2007) 1169–1181.
[22] S. Ueno, H. Yamada, T. Moriyama, et al., Measurement of dorsal root ganglion P2X mRNA by SYBR Green fluorescence, Brain Res. Brain Res. Protoc. 10 (2002) 95–101.
[23] R.H. Lekanne Deprez, A.C. Fijnvandraat, J.M. Ruijter, A.F. Moorman, Sensitivity and accuracy of quantitative real-time polymerase chain reaction using SYBR green I depends on cDNA synthesis conditions, Anal. Biochem. 307 (2002) 63–69.
[24] K.J. Livak, T.D. Schmittgen, Analysis of relative gene expression data using real-time quantitative PCR and the 2(-Delta Delta C(T)) Method, Methods 25 (2001) 402–408.
[25] A. Adhikari, C.A. Penatti, R.R. Resende, H. Ulrich, L.R. Britto, E.J. Bechara, 5-Aminolevulinate and 4,5-dioxovalerate ions decrease GABA(A) receptor density in neuronal cells, synaptosomes and rat brain, Brain Res. 1093 (2006) 95–104.
[26] C.L. Curl, C.J. Bellair, T. Harris, B.E. Allman, P.J. Harris, A.G. Stewart, A. Roberts, K.A. Nugent, L.M.D. Delbridge, Refractive index measurement in viable cells using quantitative phase-amplitude microscopy and confocal microscopy, Cytometry Part A 65[a] (2005) 88–92.
[27] M.B. Hallett, R.L. Dormer, A.K. Campbell, in: K. Siddle, J.C. Hutton (Eds.), Peptide Hormone Action, A Practical Approach, Oxford University Press, New York, 1990, pp. 115–150.
[28] A. Minta, J.P.Y. Kao, R.Y. Tsien, Fluorescent indicators for cytosolic Ca^{2+} based on rhodamine and fluorescein chromophores, J. Biol. Chem. 264 (1989) 8171–8178.
[29] G. Sharma, S. Vijayaraghavan, Nicotinic cholinergic signaling in hippocampal astrocytes involves calcium-induced calcium release from intracellular stores, Proc. Natl. Acad. Sci. U.S.A. 98 (2001) 4148–4153.
[30] L. Walch, J.P. Gascard, E. Dulmet, C. Brink, X. Norel, Evidence for a M(1) muscarinic receptor on the endothelium of human pulmonary veins, Br. J. Pharmacol. 130 (2000) 73–78.
[31] L.A. Fieber, D.J. Adams, Acetylcholine-evoked currents in cultured neurons dissociated from rat parasympathetic cardiac ganglia, J. Physiol. 434 (1991) 215–237.
[32] N.J. Buckley, T.I. Bonner, C.M. Buckley, M.R. Brann, Antagonist binding properties of five cloned muscarinic receptors expressed in CHO-K1 cell, Mol. Pharmacol. 35 (1989) 469–476.
[33] M.P. Caulfield, N.J.M. Birdsall, International Union of Pharmacology. XVII. Classification of muscarinic acetylcholine receptors, Pharmacol. Rev. 50 (1998) 279–290.
[34] A.D. Michel, R.E. Delmendo, M. Lopez, R.L. Whiting, On the interaction of gallamine with muscarinic receptor subtypes, Eur. J. Pharmacol. 182 (1990) 335–345.
[35] C.J. Doelman, R.C. Sprong, J.E. Nagtegaal, J.F. Rodrigues de Miranda, A. Bast, Prejunctional muscarinic receptors on cholinergic nerves in guinea pig airways are of the M2 subtype, Eur. J. Pharmacol. 193 (1991) 117–119.
[36] M. Jolkkonen, P.L. van Giersbergen, U. Hellman, C. Wernstedt, E. Karlsson, A toxin from the green mamba *Dendroaspis angusticeps*: amino acid sequence and selectivity for muscarinic m4 receptors, FEBS Lett. 352 (1994) 91–94.

[37] M.C. Olianas, A. Adem, E. Karlsson, P. Onali, Rat striatal muscarinic receptors coupled to the inhibition of adenylyl cyclase activity: potent block by the selective m4 ligand muscarinic toxin 3 (MT3), Br. J. Pharmacol. 118 (1996) 283–288.
[38] D.I. Yule, J.A. Williams, U73122 inhibits Ca^{2+} oscillations in response to cholecystokinin and carbachol but not to JMV-180 in rat pancreatic acinar cells, J. Biol. Chem. 267 (1992) 13830–13835.
[39] M. Suzuki, K. Muraki, Y. Imaizumi, M. Watanabe, Cyclopiazonic acid, an inhibitor of the sarcoplasmic reticulum Ca(2+)-pump, reduces Ca(2+)-dependent K+ currents in guinea-pig smooth muscle cells, Br. J. Pharmacol. 107 (1992) 134–140.
[40] N. Demaurex, D.P. Lew, K.H. Krause, Cyclopiazonic acid depletes intracellular Ca^{2+} stores and activates an influx pathway for divalent cations in HL-60 cells, J. Biol. Chem. 267 (1992) 2318–2324.
[41] S.C. Taylor, C. Peers, Store-operated Ca^{2+} influx and voltage-gated Ca^{2+} channels coupled to exocytosis in pheochromocytoma (PC12) cells, J. Neurochem. 73 (1999) 874–880.
[42] J. Gafni, J.A. Munsch, T.H. Lam, M.C. Catlin, L.G. Costa, T.F. Molinski, I.N. Pessah, Xestospongins: potent membrane permeable blockers of the inositol 1,4,5-triphosphate receptor, Neuron 19 (1997) 723–733.
[43] C.C. Felder, Muscarinic acetylcholine receptors: signal transduction through multiple effectors, FASEB J. 9 (1995) 619–625.
[44] A. Beck, R.Z. Nieden, H.P. Schneider, J.W. Deitmer, Calcium release from intracellular stores in rodent astrocytes and neurons in situ, Cell Calcium 35 (2004) 47–58.
[45] J. Meldolesi, Rapidly exchanging Ca^{2+} stores in neurons: molecular, structural and functional properties, Prog. Neurobiol. 65 (2001) 309–338.
[46] G. Dayanithi, I. Mechaly, C. Viero, et al., Intracellular Ca^{2+} regulation in rat motoneurons during development, Cell Calcium 39 (2006) 237–246.
[47] J. Rohwedel, V. Maltsev, E. Bober, H.H. Arnold, J. Hescheler, A.M. Wobus, Muscle cell differentiation of embryonic stem cells reflects myogenesis in vivo: developmentally regulated expression of myogenic determination genes and functional expression of ionic currents, Dev. Biol. 164 (1994) 87–101.
[48] J. Fuentealba, R. Olivares, E. Ales, et al., A choline-evoked $[Ca^{2+}]_i$ signal causes catecholamine release and hyperpolarization of chromaffin cells, FASEB J. 18 (2004) 1468–1470.
[49] J.K. Blusztajn, J.M. Cermak, T. Holler, D.A. Jackson, Imprinting of hippocampal metabolism of choline by its availability during gestation: implications for cholinergic neurotransmission, J. Physiol. Paris 92 (1998) 199–203.
[50] W. Marszalec, J.Z. Yeh, T. Narahashi, Desensitization of nicotine acetylcholine receptors: modulation by kinase activation and phosphatase inhibition, Eur. J. Pharmacol. 514 (2005) 83–90.
[51] J. Trouslard, S.J. Marsh, D.A. Brown, Calcium entry through nicotinic receptor channels and calcium channels in cultured rat superior cervical ganglion cells, J. Physiol. Lond. 468 (1993) 53–71.
[52] P. Seguela, J. Wadiche, K. Dineley-Miller, J.A. Dani, J.W. Patrick, Molecular cloning, functional properties, and distribution of rat brain α7: a nicotinic cation channel highly permeable to calcium, J. Neurosci. 13 (1993) 596–604.
[53] D.S. McGehee, L.W. Role, Physiological diversity of nicotinic acetylcholine receptors expressed by vertebrate neurons, Annu. Rev. Physiol. 57 (1995) 521–546.
[54] S. Vijayaraghavan, P.C. Pugh, Z.W. Zhang, M.M. Rathouz, D.K. Berg, Nicotinic receptors that bind α-bungarotoxin on neurons raise intracellular free Ca^{2+}, Neuron 8 (1992) 353–362.
[55] M.M. Rathouz, D.K. Berg, Synaptic-type acetylcholine receptors raise intracellular calcium levels in neurons by two mechanisms, J. Neurosci. 14 (1994) 6935–6945.
[56] M.J. Berridge, Neuronal calcium signaling, Neuron 21 (1998) 3–26.
[57] F. Mori, M. Fukaya, H. Abe, K. Wakabayashi, M. Watanabe, Developmental changes in expression of the three ryanodine receptor mRNAs in the mouse brain, Neurosci. Lett. 285 (2000) 57–60.
[58] F.A. Dajas-Bailador, A.J. Mogg, S. Wonnacott, Intracellular Ca^{2+} signals evoked by stimulation of nicotinic acetylcholine receptors in SH-SY5Y cells: contribution of voltage-operated Ca^{2+} channels and Ca^{2+} stores, J. Neurochem. 81 (2002) 606–614.
[59] C. Camello, R. Lomax, O.H. Petersen, A.V. Tepikin, Calcium leak from intracellular stores—the enigma of calcium signalling, Cell Calcium 32 (2002) 355–361.
[60] F. Wissing, E.P. Nerou, C.W. Taylor, A novel Ca^{2+}-induced Ca^{2+} release mechanism mediated by neither inositol triphosphate nor ryanodine receptors, Biochem. J. 361 (2002) 605–611.
[61] N. Solovyova, N. Veselovsky, E.C. Toescu, A. Verkhratsky, Ca^{2+} dynamics in the lumen of the endoplasmic reticulum in sensory neurons: direct visualization of Ca^{2+}-induced Ca^{2+} release triggered by physiological Ca^{2+} entry, EMBO J. 21 (2002) 622–630.
[62] A. Verkhratsky, A. Shmigol, Calcium-induced calcium release in neurons, Cell Calcium 19 (1996) 1–14.
[63] S. Foucart, S.J. Gibbons, J.R. Brorson, R.J. Miller, Increase in $[Ca^{2+}]_i$ by CCh in adult rat sympathetic neurons are not dependent on intracellular Ca^{2+} pools, Am. J. Physiol. 268 (1995) 829–837.
[64] C. Zhou, Z.X. Wen, D.M. Shi, Z.P. Xie, Muscarinic acetylcholine receptors involved in the regulation of neural stem cell proliferation and differentiation in vitro, Cell. Biol. Int. 28 (2004) 63–67.
[65] W.A. Staines, J. Craig, K. Reuhl, M.W. McBurney, Retinoic acid treated P19 embryonal carcinoma cells differentiate into oligodendrocytes capable of myelination, Neuroscience 71 (1996) 845–853.